

SCIENTIFIC REPORTS

OPEN

Mesoproterozoic juvenile crust in microcontinents of the Central Asian Orogenic Belt: evidence from oxygen and hafnium isotopes in zircon

Zhen-Yu He^{1,2}, Reiner Klemd², Li-Li Yan^{1,2}, Tian-Yu Lu¹ & Ze-Ming Zhang¹

We report *in situ* O and Hf isotope data of zircon grains from coeval Mesoproterozoic (ca. 1.4 Ga) igneous metamafic (amphibolite) and granitic rocks of the Chinese Central Tianshan microcontinent (CTM) in the southern Central Asian Orogenic Belt (CAOB). Zircon grains from amphibolite have mantle-like $\delta^{18}\text{O}_{\text{VSMOW}}$ values of 4.7–5.6‰ and juvenile Hf isotopic compositions ($\epsilon_{\text{Hf}}(t) = 8.4\text{--}15.3$; $T_{\text{DMC}} = 1.57\text{--}1.22$ Ga), whereas those from granitic rocks have $\delta^{18}\text{O}_{\text{VSMOW}}$ values of 5.6–7.0‰ and evolved Hf isotopic compositions ($\epsilon_{\text{Hf}}(t) = -1.0\text{--}8.2$; $T_{\text{DMC}} = 2.09\text{--}1.62$ Ga). Zircon O–Hf isotopic compositions of the metamafic and granitic rocks provide evidence for Mesoproterozoic (ca. 1.4 Ga) crustal growth and a substantial Palaeoproterozoic supracrustal component in the CTM. These findings and previous studies, reporting ca. 1.4 Ga magmatic rocks from other microcontinents of the CAOB, suggest that a large belt of Mesoproterozoic (ca. 1.4 Ga) juvenile continental crust formed in a continental terrane, fragments of which now occur over a distance of more than a thousand kilometres in the southern CAOB.

The Central Asian Orogenic Belt (CAOB), one of the largest Neoproterozoic to Palaeozoic accretionary orogens on Earth, has been extensively studied in order to constrain juvenile continental crustal growth during the Phanerozoic^{1–4}. Microcontinents with Precambrian crystalline basement are essential components of the CAOB by constituting approximately 50% of its crust⁵. However, their geological evolution is only poorly constrained due to restricted exposure of the Precambrian rocks, which were extensively overprinted by Palaeozoic tectonic, metamorphic and magmatic events and were largely incorporated into Palaeozoic magmatic arcs^{6–9}. Therefore, deciphering the crustal components of these microcontinents is critical to constrain juvenile continental growth in the CAOB. Recently, *in situ* zircon geochronology confirmed Mesoproterozoic (ca. 1.4 Ga) magmatic activity in the CAOB, which undoubtedly testifies to the occurrence of continental crust generated before amalgamation of the CAOB (Table 1)^{7,10–16}. The Mesoproterozoic Era, dominated by the break-up of the Columbia supercontinent and the formation of the Rodinia supercontinent, was an important crust-forming period in many continents across the world^{17–19}. But the best-preserved remnants of ca. 1.4 Ga juvenile crust occur in eastern Laurentia, SW Baltica and SW Amazonia^{20–23}. In this context, Mesoproterozoic (ca. 1.4 Ga) magmatism is critical to clarify the crustal evolution of the host microcontinents in the CAOB (cf. ref.⁸).

However, whether ca. 1.4 Ga magmatism in the microcontinents of the CAOB was actually accompanied by significant crustal growth has largely remained speculative up to now, since the zircon Hf isotope signatures and bulk compositions of the magmatic rocks preclude derivation directly from the mantle^{7,10–13,16}. However, zircon oxygen isotopic compositions are particularly useful for determining the origin of magmatic rocks since zircon in equilibrium with mantle-derived melts has a narrow $\delta^{18}\text{O}_{\text{VSMOW}}$ range [$5.3 \pm 0.6\text{‰}$ (2SD)], which is thought to be insensitive to magmatic differentiation^{24–26}. In contrast, zircon crystallized in magma from a supracrustal source has elevated $\delta^{18}\text{O}$ values. Zircon oxygen isotopic compositions can also be used to track the isotopic evolution of a

¹Key Laboratory of Deep-Earth Dynamics, Institute of Geology, Chinese Academy of Geological Sciences, 26 Baiwanzhuang Road, Beijing, 100037, China. ²GeoZentrum Nordbayern, Friedrich-Alexander Universität Erlangen-Nürnberg, Schlossgarten 5, D-91054, Erlangen, Germany. Correspondence and requests for materials should be addressed to Z.-Y.H. (email: ahzy@163.com)

Tectonic unit	locality	Lithology	Age (Ma)	$\epsilon_{\text{Hf}}(t)$	T_{DMC} (Ga)	Data source
Chinese Central Tianshan	Alatage	amphibolite	1384 ± 35	8.4–15.3	1.57–1.22	This study
	Alatage	gneissic granodiorite	1437 ± 4	2.2–6.5	1.93–1.71	ref. ⁷
	Alatage	gneissic granodiorite	1438 ± 5	1.5–6.2	1.97–1.73	ref. ⁷
	Alatage	gneissic monzogranite	1436 ± 4	4.2–8.2	1.83–1.62	ref. ⁷
	Alatage	gneissic monzogranite	1436 ± 5	0.4–5.3	2.02–1.77	ref. ⁷
	Alatage	gneissic tonalites	1436 ± 5	3.1–7.7	1.88–1.65	ref. ⁷
	Alatage	gneissic tonalites	1436 ± 5	−1.0–6.8	2.09–1.70	ref. ⁷
	Alatage	gneissic tonalites	1436 ± 5	2.0–7.6	1.94–1.65	ref. ⁷
	Weiya	granitic gneiss	1433 ± 27	0.3–7.0	2.02–1.68	ref. ⁷
	Xingxingxia	granitic gneiss	1409 ± 33	−0.2–8.6	2.03–1.58	ref. ⁷
Beishan	Jiuqing	granitic gneiss	1408 ± 4	2.7–12.4	2.00–1.38	ref. ¹⁰
Xilinhot block	Sonid Zuoqi	granitic gneiss	1390 ± 17	0.4–12.0	1.98–1.39	ref. ¹¹
	Sonid Zuoqi	granitic gneiss	1397 ± 11			ref. ¹²
	Sonid Zuoqi	granitic gneiss	1371 ± 9			ref. ¹²
	Sonid Zuoqi	granitic gneiss	1369 ± 11			ref. ¹²
	Sonid Zuoqi	granitic gneiss	1360 ± 12			ref. ¹²
Alxa block	Zongnaishan	granitic gneiss	1433 ± 17	0.1–11.9	2.19–1.44	ref. ¹³
Kyrgyz North Tianshan	Makbal	eclogite	1446 ± 25*			ref. ¹⁴
	Makbal	eclogite	1447 ± 29*			ref. ¹⁴
	Aktyuz	rhyolite	1373 ± 5*			ref. ¹⁶
	Aktyuz	rhyolite	1365 ± 6*			ref. ¹⁶

Table 1. Compilation of sample locations, ages and zircon Hf isotopic compositions of the Mesoproterozoic magmatic rocks from microcontinents in the southern CAOB. The star (*) indicates SHRIMP zircon U–Pb ages; the others are LA-ICP-MS zircon U–Pb ages.

magmatic system through inter- or intragrain variations due to the long residence time of zircon in magma chambers^{25–27}. In this study, we present *in situ* O and Hf isotope compositions of zircon grains from Mesoproterozoic magmatic metamafic and granitic rocks from the Alatage area in the Chinese Central Tianshan microcontinent (CTM) of the southern CAOB to gain insight into crustal evolution of the CTM (Fig. 1). The new data allow us to propose Mesoproterozoic (ca. 1.4 Ga) juvenile magmatism in the microcontinents of the southern CAOB.

Results

Field occurrence and petrography. The Chinese Tianshan is commonly subdivided into the North Tianshan, the Yili block, the CTM and the South Tianshan Accretionary Complex, and occupies major parts of the southwestern CAOB^{28–30}. A Palaeozoic continental arc with Precambrian basement characterizes the CTM. The basement rocks are mainly exposed in the Xingxingxia, Weiya, Alatage and Baluntai areas and include Mesoproterozoic igneous and supracrustal rocks that were ascribed to the Xingxingxia Group^{6,7,31,32}.

The Alatage metamafic rocks occur as boudins and lenses ranging from metres to tens of metres in length in Palaeozoic mylonitic granitoids and are commonly aligned with the foliation (Fig. 1b). The investigated amphibolite sample X15–54 is predominantly composed of hornblende (~60 vol.%) and plagioclase (~30 vol.%), with minor biotite, magnetite and quartz. The rock has a protolith age of 1384 ± 35 Ma (Table S1; Figs S1 and S2). The Mesoproterozoic granitic rocks in the Alatage area intruded into marble and schist of the Xingxingxia Group and were in turn intruded by Palaeozoic granitoids, occurring as sporadic outcrops (Fig. 1b). The gneissic granitoids are mylonitized to a varying extent and classify as granite, granodiorite, tonalite and quartz diorite (see details in ref.⁷). The granitic rocks were emplaced almost synchronously with the protolith of the amphibolites and have zircon crystallization ages of ca. 1438–1436 Ma⁷.

Zircon O isotopes. Fifteen analyses on fifteen magmatic zircon grains from amphibolite sample X15–54 show limited intragrain O isotope variability. The $\delta^{18}\text{O}_{\text{VSMOW}}$ values cluster between 4.7 and 5.6‰, with an average of $5.2 \pm 0.5\text{‰}$ (2 SD; Fig. 2). In addition, fifteen analyses on 15 magmatic zircon grains from gneissic granodiorite sample X12–38 revealed $\delta^{18}\text{O}_{\text{VSMOW}}$ values of 5.6 to 7.0‰, with an average of $6.5 \pm 0.9\text{‰}$ (2 SD; Fig. 2). This intragrain $\delta^{18}\text{O}$ range distinctly exceeds that of the homogeneous zircon standard Penglai (0.5‰; Table S2).

Zircon Hf isotopic compositions. Eight Lu–Hf analyses were performed on 8 magmatic zircon grains from amphibolite sample X15–54. These analyses commonly show uniform initial $^{176}\text{Hf}/^{177}\text{Hf}$ ratios of 0.282142 to 0.282337 (Fig. 3), that correspond to $\epsilon_{\text{Hf}}(t)$ values between 8.4 and 15.3 and crustal model ages (T_{DMC}) of 1.57 to 1.22 Ga (Table S3). The zircon Hf data for the Alatage granitic rocks, which include gneissic granodiorite sample X12–38, were described in detail in ref.⁷. A total of 120 Hf isotopic spot analyses on zircon grains from seven samples yielded varying initial $^{176}\text{Hf}/^{177}\text{Hf}$ ratios from 0.281844 to 0.282103 and $\epsilon_{\text{Hf}}(t)$ values from −1.0 to 8.2, corresponding to crustal model ages (T_{DMC}) of 2.09 Ga to 1.62 Ga (Fig. 3).

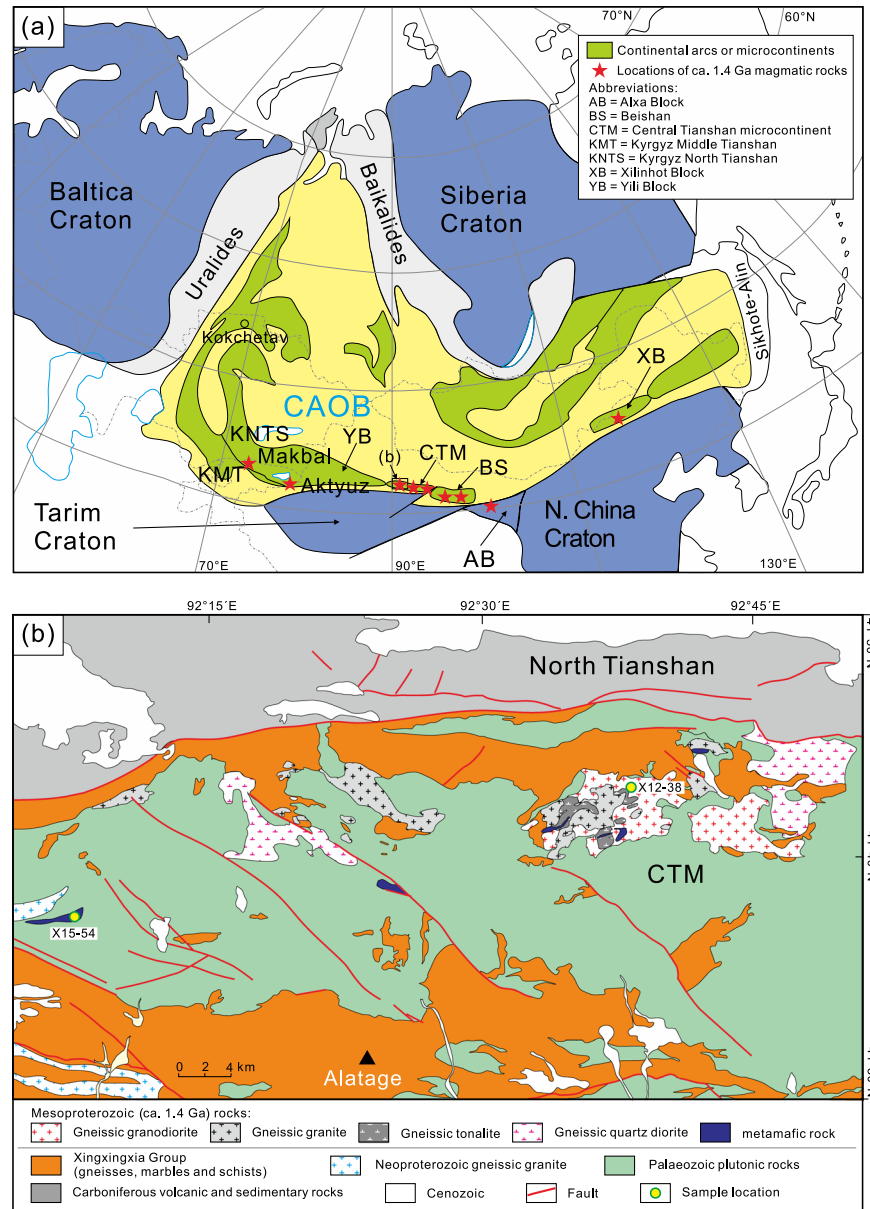


Figure 1. (a) Simplified geological map of the Central Asian Orogenic Belt. The distributions of the ca. 1.4 Ga magmatic rocks are displayed by red stars (Data sources: refs^{7,10–16}). The major microcontinents in the Central Asian Orogenic Belt are also indicated, including, from west to east, the Kazakhstan, Yili, Central Tianshan, Beishan, Tuva-Mongolia and NE China microcontinental collages. (b) Simplified geological map of the Alatage area, showing the distribution and outline of Mesoproterozoic igneous rocks in this area. This figure was generated by Z.Y.H. using CorelDRAW 2017 (<https://www.coreldraw.com/en/pages/free-download/>).

Discussion

Mesoproterozoic crustal growth and nature of crustal components in the CTM. The Alatage amphibolite shows primitive zircon oxygen isotopic compositions with zircon $\delta^{18}\text{O}_{\text{VSMOW}}$ values identical to those of zircon in equilibrium with mantle-derived melts (Fig. 2). The zircon Hf isotopic compositions are radiogenic and overlap the depleted mantle line (Fig. 3). The coupling of zircon O and Hf isotope compositions implies that the parental magma of the Alatage amphibolite protolith was ultimately derived from the depleted mantle, which is also in accordance with its mafic character ($\text{SiO}_2 = 50.8 \text{ wt.}\%$). In contrast, the Alatage granitic rocks show somewhat evolved Hf isotope signatures with Palaeoproterozoic T_{DMC} crustal model ages (2.09 to 1.62 Ga) that are commonly older than the crystallization ages (Fig. 3; the difference is approximately 0.20 to 0.70 Ga), suggesting a mixed juvenile and recycled (metasedimentary) source or an ancient mantle-derived source (infracrustal progenitor)^{24–26}. Besides, they exhibit a large range in zircon $\delta^{18}\text{O}_{\text{VSMOW}}$ values from a mantle-like value to high $\delta^{18}\text{O}_{\text{VSMOW}}$ values representative of recycling of sedimentary material (Fig. 2). Thus, the magma of the Alatage granitic rocks is thought to have been derived from a mixed sedimentary source and mantle melts, and thus their Hf model ages (2.09 to 1.62 Ga) may be hybrid, reflecting mixing rather than specific crust-forming

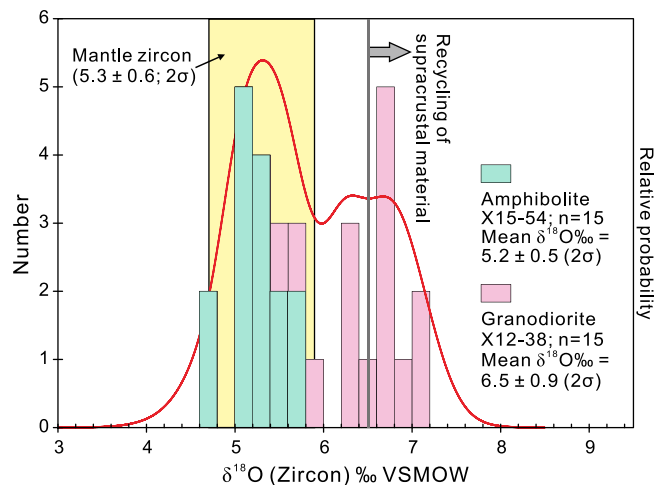


Figure 2. Histogram showing zircon $\delta^{18}\text{O}_{\text{VSMOW}}$ values for the ca. 1.4 Ga Alatage amphibolite and gneissic granodiorite. Yellow bar represents $\delta^{18}\text{O}_{\text{VSMOW}}$ of zircon in equilibrium with mantle-derived melts ($5.3 \pm 0.6\text{‰}$, 2σ); values above 6.5‰ indicate recycling of supracrustal material^{24–26}. Note the amphibolite has broadly mantle-like zircon $\delta^{18}\text{O}$ values, while the zircon $\delta^{18}\text{O}_{\text{VSMOW}}$ values of the gneissic granodiorite are relative high and variable.

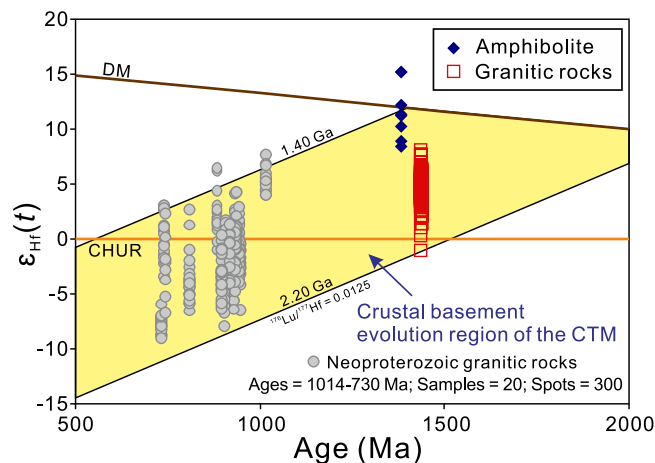


Figure 3. Zircon Hf isotopic evolution diagram for the ca. 1.4 Ga Alatage amphibolite and granitic rocks. Also showing the Neoproterozoic granitic rocks from the CTM (Data sources: refs.^{6,7,33–40}). Note that the $\epsilon_{\text{Hf}}(t)$ values of the Neoproterozoic granitic rocks are typically located in the crustal basement evolution region of the CTM as defined by the Mesoproterozoic rocks. The ‘crust evolution curve’ is based on the $^{176}\text{Lu}/^{177}\text{Hf}$ value of 0.0125 for average upper continental crust⁴⁹.

events. However, a supracrustal component with an age of at least 1.62 Ga was deduced in the crust of the CTM. In summary, zircon O–Hf isotope compositions of the Alatage metamorphic and granitic rocks reveal evidence for Mesoproterozoic (ca. 1.4 Ga) crustal growth and a possible Palaeoproterozoic supracrustal component in the CTM. Moreover, Neoproterozoic granitic rocks with protolith crystallization ages between ca. 1014 and 730 Ma are also abundant in the CTM^{6,7,33–40}. Their $\epsilon_{\text{Hf}}(t)$ values are typically located in crustal evolution region of the CTM as defined by Mesoproterozoic rocks (Fig. 3). This indicates that the Palaeoproterozoic supracrustal component and the Mesoproterozoic juvenile crust of the CTM were reworked in the Neoproterozoic.

Mesoproterozoic (ca. 1.4 Ga) juvenile continental crust and its fragments in the southern CAOB. Mesoproterozoic magmatic events were recently identified in several microcontinents of the southern CAOB (Table 1). The present findings reveal evidence for Mesoproterozoic (ca. 1.4 Ga) crustal growth in the Alatage area of the CTM. Similar Mesoproterozoic magmatic activity at ca. 1.43–1.41 Ga involving juvenile crustal growth also occurred in the Weiya and Xingxingxia areas of the CTM with $\epsilon_{\text{Hf}}(t)$ values from -0.2 to 8.6 and T_{DMC} crustal model ages of 2.03 to 1.58 Ga⁷. In addition, gneissic granitoids with a protolith age of 1408 ± 4 Ma were reported from the Beishan microcontinent to the east of the CTM¹⁰. Their radiogenic Hf isotopic compositions ($\epsilon_{\text{Hf}}(t) = 2.7–12.4$; $T_{\text{DMC}} = 2.00–1.38$ Ga) indicate the involvement of juvenile crust¹⁰. Furthermore, Mesoproterozoic (1.39–1.36 Ga) granitic rocks and associated crustal growth events were reported from the

Xilinhot block in the eastern CAOB with $\varepsilon_{\text{Hf}}(t)$ values from 0.4 to 12.0 and T_{DMC} model ages of 1.98 to 1.39 Ga^{11,12}. Similarly, Mesoproterozoic granitic rocks with an age of 1433 ± 17 Ma also occur in the northern Alxa block on the southeastern margin of the CAOB, and their Hf crustal model ages (2.19–1.44 Ga) suggest the involvement of juvenile material in their magma sources¹³. In particular, magmatic protolith ages of 1446 ± 25 Ma and 1447 ± 29 Ma were reported for eclogite-facies rocks from the Makbal metamorphic complex in the Kyrgyz North Tianshan, western CAOB^{14,15}. Mesoproterozoic (1373–1365 Ma) volcanic rocks also occur in the Aktuz area of the Kyrgyz North Tianshan¹⁶. Therefore, it is suggested that Mesoproterozoic (ca. 1.4 Ga) juvenile continental crust probably occurred along a large continental belt, now largely tectonically fragmented, ranging from the Kyrgyz North and Middle Tianshan through the Yili, Central Tianshan, Beishan and northern Alxa blocks or microcontinents in NW China to the Xilinhot block in NE China (Fig. 1a). The microcontinents are believed to have formed as part of a continental terrane, fragments of which now occur over a distance of more than a thousand kilometres in the southern CAOB. The previously unknown ca. 1.4 Ga continental crustal growth episode is a remarkable feature of the microcontinents in the CAOB and may provide important clues for the origin and evolution of the host microcontinents and thus the reconstruction of tectonic environments in the CAOB.

Methods

Zircon O isotopes. Zircon oxygen isotopes were measured using the Cameca 1280 SIMS at Institute of Geology and Geophysics, Chinese Academy of Sciences, Beijing. The Cs⁺ primary ion beam was accelerated at 10 kV with an intensity of ca. 2 nA. The spot diameters were ca. 10 μm . The instrumental mass fractionation factor (IMF) was corrected using the Penglai zircon standard ($\delta^{18}\text{O}_{\text{VSMOW}} = 5.3\%$)⁴¹. The detailed analytical procedures have been described in ref.⁴¹. The two standard deviation of the reproducibility of the Penglai zircon standard during the course of this study was 0.5‰ (2 SD; $n = 23$; Table S2), which accounts for the analytical precision. Eleven analyses of in-house zircon standard Qinghu during the course of this study yield a weighted mean of $\delta^{18}\text{O} = 5.4 \pm 0.7\%$ (2 SD; Table S2), which is consistent within errors with the reported value of $5.4 \pm 0.2\%$ ⁴².

Zircon Hf isotopic compositions. Zircon Hf isotope analyses were carried out *in situ* using a Coherent GeoLas Pro 193-nm laser ablation system combined with a Thermo Scientific Neptune Plus Multi Collector ICP-MS at the State Key Laboratory for Mineral Deposits Research, Nanjing University. Analyses were carried out with a beam diameter of 44 μm . The detailed procedure and interference correction method of ¹⁷⁶Yb on ¹⁷⁶Hf are described in ref.⁴³. Standard Mud Tank was analysed during the course of this study and yielded a mean ¹⁷⁶Hf/¹⁷⁷Hf value of 0.282493 ± 44 (2 SD; $n = 59$; Table S3), which is consistent within error with the recommended values⁴⁴. The measured ¹⁷⁶Lu/¹⁷⁷Hf ratios and the ¹⁷⁶Lu decay constant of $1.867 \times 10^{-11} \text{ yr}^{-1}$ were used to calculate initial ¹⁷⁶Hf/¹⁷⁷Hf ratios⁴⁵. The chondritic values of ref.⁴⁶ were used for the calculation of the ε_{Hf} values. The depleted mantle Hf model age (T_{DM}) was calculated using the analysed ¹⁷⁶Lu/¹⁷⁷Hf value of zircon and depleted mantle values of ref.⁴⁷. The crustal model age (T_{DMC}) was calculated using a ¹⁷⁶Lu/¹⁷⁷Hf value of 0.022 for mafic rocks and 0.009 for felsic rocks⁴⁸.

References

- Şengör, A. M. C., Natal'in, B. A. & Burtman, V. S. Evolution of the Altaid tectonic collage and Palaeozoic crustal growth in Eurasia. *Nature* **364**, 299–307 (1993).
- Jahn, B., Wu, F. & Chen, B. Massive granitoid generation in Central Asia: Nd isotope evidence and implication for continental growth in the Phanerozoic. *Episodes* **23**, 82–92 (2000).
- Xiao, W. *et al.* Palaeozoic accretionary and convergent tectonics of the southern Altai: implications for the growth of Central Asia. *Journal of the Geological Society* **161**, 339–342 (2004).
- Tang, G.-J. *et al.* Short episodes of crust generation during protracted accretionary processes: evidence from Central Asian Orogenic Belt, NW China. *Earth and Planetary Science Letters* **464**, 142–154 (2017).
- Kovalenko, V. I. *et al.* Isotope provinces, mechanisms of generation and sources of the continental crust in the Central Asian mobile belt: geological and isotopic evidence. *Journal of Asian Earth Sciences* **23**, 605–627 (2004).
- He, Z.-Y. *et al.* Zircon U–Pb and Hf isotopic studies of the Xingxingxia Complex from Eastern Tianshan (NW China): significance to the reconstruction and tectonics of the southern Central Asian Orogenic Belt. *Lithos* **190**, 485–499 (2014).
- He, Z.-Y. *et al.* Mesoproterozoic continental arc magmatism and crustal growth in the eastern Central Tianshan Arc Terrane of the southern Central Asian Orogenic Belt: geochronological and geochemical evidence. *Lithos* **236**, 74–89 (2015).
- Kröner, A. *et al.* No excessive crustal growth in the Central Asian Orogenic Belt: further evidence from field relationships and isotopic data. *Gondwana Research* **50**, 135–166 (2017).
- Degtyarev, K., Yakubchuk, A., Tretyakov, A., Kotov, A. & Kovach, V. Precambrian geology of the Kazakh uplands and Tien Shan: an overview. *Gondwana Research* **47**, 44–75 (2017).
- He, Z., Sun, L., Mao, L., Zong, K. & Zhang, Z. Zircon U–Pb and Hf isotopic study of gneiss and granodiorite from the southern Beishan orogenic collage: Mesoproterozoic magmatism and crustal growth. *Chinese Science Bulletin* **60**, 389–399 (2015).
- Sun, L. X. *et al.* Zircon U–Pb dating and Hf isotopic compositions of the Mesoproterozoic granitic gneiss in Xilinhot Block, Inner Mongolia. *Geological Bulletin of China* **32**, 327–340 (2013).
- Han, J., Zhou, J.-B., Li, L. & Song, M.-C. Mesoproterozoic (~1.4 Ga) A-type gneissic granites in the Xilinhot terrane, NE China: first evidence for the break-up of Columbia in the eastern CAOB. *Precambrian Research* **296**, 20–38 (2017).
- Shi, X. J. *et al.* Zircon geochronology and Hf isotopic compositions for the Mesoproterozoic gneisses in Zongnaishan area, northern Alxa and its tectonic affinity. *Acta Petrologica Sinica* **32**, 3518–3536 (2016).
- Konopelko, D. *et al.* SHRIMP zircon chronology of HP–UHP rocks of the Makbal metamorphic complex in the Northern Tien Shan, Kyrgyzstan. *Gondwana Research* **22**, 300–309 (2012).
- Konopelko, D. & Klemd, R. Deciphering protoliths of the (U) HP rocks in the Makbal metamorphic complex, Kyrgyzstan: geochemistry and SHRIMP zircon geochronology. *European Journal of Mineralogy* **28**, 1233–1253 (2016).
- Kröner, A. *et al.* Mesoproterozoic (Grenville-age) terranes in the Kyrgyz North Tianshan: zircon ages and Nd–Hf isotopic constraints on the origin and evolution of basement blocks in the southern Central Asian Orogen. *Gondwana Research* **23**, 272–295 (2013).
- Rogers, J. J. & Santosh, M. Configuration of Columbia, a Mesoproterozoic supercontinent. *Gondwana Research* **5**, 5–22 (2002).
- Zhao, G., Sun, M., Wilde, S. A. & Li, S. A Paleo-Mesoproterozoic supercontinent: assembly, growth and breakup. *Earth-Science Reviews* **67**, 91–123 (2004).
- Roberts, N. M. W., Slagstad, T. & Viola, G. The structural, metamorphic and magmatic evolution of Mesoproterozoic orogens. *Precambrian Research* **265**, 1–9 (2015).

20. Andersen, T., Griffin, W. L. & Pearson, N. J. Crustal evolution in the SW part of the Baltic Shield: the Hf isotope evidence. *Journal of Petrology* **43**, 1725–1747 (2002).
21. Rämö, O. T. *et al.* Intermittent 1630–1220 Ma magmatism in central Mazatzal Province: new geochronologic piercing points and some tectonic implications. *Geology* **31**, 335–338 (2003).
22. Goodge, J. W. & Vervoort, J. D. Origin of Mesoproterozoic A-type granites in Laurentia: Hf isotope evidence. *Earth and Planetary Science Letters* **243**, 711–731 (2006).
23. Bettencourt, J. S. *et al.* The Rondonian-San Ignacio Province in the SW Amazonian Craton: an overview. *Journal of South American Earth Sciences* **29**, 28–46 (2010).
24. Valley, J. W. *et al.* 4.4 billion years of crustal maturation: oxygen isotope ratios of magmatic zircon. *Contrib Mineral Petrol* **150**, 561–580 (2005).
25. Hawkesworth, C. J. & Kemp, A. I. S. Using hafnium and oxygen isotopes in zircons to unravel the record of crustal evolution. *Chemical Geology* **226**, 144–162 (2006).
26. Kemp, A. I. S. *et al.* Magmatic and crustal differentiation history of granitic rocks from Hf–O isotopes in zircon. *Science* **315**, 980–983 (2007).
27. Wang, X.-L. *et al.* Magmatic evolution and crustal recycling for Neoproterozoic strongly peraluminous granitoids from southern China: Hf and O isotopes in zircon. *Earth and Planetary Science Letters* **366**, 71–82 (2013).
28. Gao, J., Li, M., Xiao, X., Tang, Y. & He, G. Paleozoic tectonic evolution of the Tianshan Orogen, northwestern China. *Tectonophysics* **287**, 213–231 (1998).
29. Gao, J. *et al.* Tectonic evolution of the South Tianshan orogen and adjacent regions, NW China: geochemical and age constraints of granitoid rocks. *International Journal of Earth Sciences* **98**, 1221–1238 (2009).
30. Xiao, W.-J., Zhang, L.-C., Qin, K.-Z., Sun, S. & Li, J.-L. Paleozoic accretionary and collisional tectonics of the Eastern Tianshan (China): implications for the continental growth of central Asia. *American Journal of Science* **304**, 370–395 (2004).
31. Hu, A., Jahn, B., Zhang, G., Chen, Y. & Zhang, Q. Crustal evolution and Phanerozoic crustal growth in northern Xinjiang: Nd isotopic evidence. Part I. Isotopic characterization of basement rocks. *Tectonophysics* **328**, 15–51 (2000).
32. Liu, S., Guo, Z., Zhang, Z., Li, Q. & Zheng, H. Nature of the Precambrian metamorphic blocks in the eastern segment of Central Tianshan: constraint from geochronology and Nd isotopic geochemistry. *Science in China Series D: Earth Sciences* **47**, 1085–1094 (2004).
33. Lei, R.-X. *et al.* Zircon U–Pb chronology and Hf isotope of the Xingxingxia granodiorite from the Central Tianshan zone (NW China): implications for the tectonic evolution of the southern Altai. *Gondwana Research* **20**, 582–593 (2011).
34. Wang, Z.-M. *et al.* The petrogenesis and tectonic implications of the granitoid gneisses from Xingxingxia in the eastern segment of Central Tianshan. *Journal of Asian Earth Sciences* **88**, 277–292 (2014).
35. Gao, J. *et al.* Record of assembly and breakup of Rodinia in the Southwestern Altai: evidence from Neoproterozoic magmatism in the Chinese Western Tianshan Orogen. *Journal of Asian Earth Sciences* **113**, 173–193 (2015).
36. Liu, Q. *et al.* Ages and tectonic implications of Neoproterozoic ortho- and paragneisses in the Beishan Orogenic Belt, China. *Precambrian Research* **266**, 551–578 (2015).
37. Huang, B., He, Z., Zong, K. & Zhang, Z. Zircon U–Pb and Hf isotopic study of Neoproterozoic granitic gneisses from the Alatai area, Xinjiang: constraints on the Precambrian crustal evolution in the Central Tianshan Block. *Chinese Science Bulletin* **59**, 100–112 (2014).
38. Huang, B.-T. *et al.* Early Neoproterozoic granitic gneisses in the Chinese Eastern Tianshan: petrogenesis and tectonic implications. *Journal of Asian Earth Sciences* **113**, 339–352 (2015).
39. Huang, Z. *et al.* Neoproterozoic granitic gneisses in the Chinese Central Tianshan Block: implications for tectonic affinity and Precambrian crustal evolution. *Precambrian Research* **269**, 73–89 (2015).
40. Huang, Z. *et al.* Precambrian evolution of the Chinese Central Tianshan Block: constraints on its tectonic affinity to the Tarim Craton and responses to supercontinental cycles. *Precambrian Research* **295**, 24–37 (2017).
41. Li, X. H. *et al.* Penglai zircon megacrysts: a potential new working reference material for microbeam determination of Hf–O isotopes and U–Pb age. *Geostandards and Geoanalytical Research* **34**, 117–134 (2010).
42. Li, X. *et al.* Qinghu zircon: A working reference for microbeam analysis of U–Pb age and Hf and O isotopes. *Chinese Science Bulletin* **58**, 4647–4654 (2013).
43. Wu, F.-Y., Yang, Y.-H., Xie, L.-W., Yang, J.-H. & Xu, P. Hf isotopic compositions of the standard zircons and baddeleyites used in U–Pb geochronology. *Chemical Geology* **234**, 105–126 (2006).
44. Woodhead, J. D. & Hergt, J. M. A preliminary appraisal of seven natural zircon reference materials for *in situ* Hf isotope determination. *Geostandards and Geoanalytical Research* **29**, 183–195 (2005).
45. Söderlund, U., Patchett, P. J., Vervoort, J. D. & Isachsen, C. E. The ^{176}Lu decay constant determined by Lu–Hf and U–Pb isotope systematics of Precambrian mafic intrusions. *Earth and Planetary Science Letters* **219**, 311–324 (2004).
46. Bouvier, A., Vervoort, J. D. & Patchett, P. J. The Lu–Hf and Sm–Nd isotopic composition of CHUR: constraints from unequilibrated chondrites and implications for the bulk composition of terrestrial planets. *Earth and Planetary Science Letters* **273**, 48–57 (2008).
47. Griffin, W. L. *et al.* The Hf isotope composition of cratonic mantle: LAM-MC-ICPMS analysis of zircon megacrysts in kimberlites. *Geochimica et Cosmochimica Acta* **64**, 133–147 (2000).
48. Gardiner, N. J., Johnson, T. E., Kirkland, C. L. & Smithies, R. H. Melting controls on the lutetium–hafnium evolution of Archaean crust. *Precambrian Research* **305**, 479–488 (2018).
49. Chauvel, C. *et al.* Constraints from loess on the Hf–Nd isotopic composition of the upper continental crust. *Earth and Planetary Science Letters* **388**, 48–58 (2014).

Acknowledgements

This work was supported by the National Key R&D Program of China (2017YFC0601206), National Natural Science Foundation of China (41772060), and Chinese Geological Survey Project (DD20160122-03).

Author Contributions

Z.Y.H. conceived the project. Z.Y.H., L.L.Y. and T.Y.L. carried out the fieldwork and performed the analytical works. Z.Y.H., R.K. and Z.M.Z. had the idea for the study. Z.Y.H. and R.K. wrote the manuscript.

Additional Information

Supplementary information accompanies this paper at <https://doi.org/10.1038/s41598-018-23393-4>.

Competing Interests: The authors declare no competing interests.

Publisher's note: Springer Nature remains neutral with regard to jurisdictional claims in published maps and institutional affiliations.



Open Access This article is licensed under a Creative Commons Attribution 4.0 International License, which permits use, sharing, adaptation, distribution and reproduction in any medium or format, as long as you give appropriate credit to the original author(s) and the source, provide a link to the Creative Commons license, and indicate if changes were made. The images or other third party material in this article are included in the article's Creative Commons license, unless indicated otherwise in a credit line to the material. If material is not included in the article's Creative Commons license and your intended use is not permitted by statutory regulation or exceeds the permitted use, you will need to obtain permission directly from the copyright holder. To view a copy of this license, visit <http://creativecommons.org/licenses/by/4.0/>.

© The Author(s) 2018